

WATER VAPOR EFFECT ON 3-5 μm Band THERMAL IMAGING IN KARBALA CITY

تأثير بخار الماء على التصوير الحراري في المدى (3-5 مايكرومتر) في مدينة كربلاء المقدسة

FADHIL K. FULIFUL

Department of Physics, College of Science, University of Karbala

E-mail: Fadhil.Khaddam@yahoo.com

1-Abstract

This paper analyzes the effect of water vapor on the accuracy of thermal images in blessed Karbala city. The distribution of water in the atmosphere varies strongly with time, location and height, which makes it difficult to model. The amounts of water vapor which are used in this research depending on the experimental data from Iraq Meteorological Organization and Seismology. The IR transmission is considered a very important parameter that has to be taken in account in thermal imaging. FORTRAN Program of an empirical expression for atmospheric attenuation as a function of wavelength and visible range in case of dust is used in this work. The IR transmissions at different extents (100,200,300,400,500,600,700,800,900m) and different concentrations of water vapor (59.1, 97.4, 167, 222.7, 310.7, 395.4, 432.9, 388.7, 300.2 mm at months JAN., FEB., MAR., APR., MAY., JUN., JUL., AUG., SEP., respectively for 2013 year) on 3-5 μm bands are calculated. The results show that at high concentration of water vapor and long distance the thermal images vanish, also at low concentration and long distance the image does not recognized.

Key words: thermal imaging, IR Bands, IR transmissions, Atmosphere Attenuation.

الخلاصة:

يحلل هذا البحث تأثير بخار الماء على دقة الصور الحرارية في مدينة كربلاء المقدسة، توزيع الماء في الغلاف الجوي يختلف بقوة مع الزمن حسب الموقع والارتفاع وبذلك نجد صعوبة في الحصول على نموذج للتوزيع كمي بخار الماء التي استخدمت في هذا البحث اعتمدت على البيانات العملية المسجلة لدى الهيئة العامة للأنواء الجوية والرصد الزلزالي العراقية. تعتبر نفاذية الأشعة تحت الحمراء عامل مهم جداً يجب ان يؤخذ في الحسبان في التصوير الحراري. استخدم في هذا العمل برنامج فورتران لعلاقة شبه تجريبية للتوهين الجوي كدالة للطول الموجي ومدى الرؤية في حالة الغبار. تم حساب نفاذية الأشعة تحت الحمراء لمديات مختلفة

(100,200,300,400,500,600,700,800,900 m) تحت تأثير تراكيز مختلفة من بخار الماء (59.1, 97.4, 167, 222.7, 310.7, 395.4, 432.9, 388.7, 300.2 mm) للشهر كانون الثاني، شباط، آذار، نيسان، أيار، حزيران، تموز، آب، أيلول على التوالي للعام 2013) وللحزم 3-5 مايكرومتر بينت النتائج في حالة التراكيز العالية والمسافات الطويلة تتلاشى الصورة الحرارية وكذلك عند التراكيز القليلة والمسافات الطويلة لا يمكن تمييز الصورة.

2-Introduction

Infrared light falls between the visible and microwave parts of the electromagnetic spectrum with wavelengths of 2-15 μm , so is not visible to the human eye. Any object with a temperature higher than absolute zero radiate energy as electromagnetic waves [1]. Most emissive power falls within the IR part of the electromagnetic spectrum, as the temperature increases, the amount of energy emitted at any wavelength increases too, and the wavelength of peak emission decreases or shifting towards the shorter wavelength region according to spectral distribution of energy in thermal radiation. To read correct temperatures, one important thing needs to be taken into account, and that is a factor known as emissivity. Emissivity is the efficiency with which an object emits infrared radiation. Thermal imaging devices make an image of the thermal patterns and

measure the emissive power of surfaces in an area at various temperatures ranges [2]. The thermal image is a measuring of temperature difference [3]. Large size particles in the atmosphere (i.e. water vapor, carbon dioxide gas molecules and ozone) attenuate radiation, since the absorption varies with the thickness of the gas traversed by the radiation [1]. There were many dedicated efforts of specialists in this field that lead to computer models of the atmosphere effects. IR Transmission of the atmosphere for a (1800 m) horizontal path at sea level containing 17 mm of precipitate water to window 3-5 μm are indicated [3]. Prediction of what happens to the thermal image due to the influence of the atmosphere parameters have been studied by a new atmospheric model, the IR transmission in the 3-5 μm band was studied using the computer code LOWTRAN6 in both the horizontal and slant path at different altitudes (0.005, 1, 2, 3, 5, 7, 10, 20 km) and ranges (1, 2, 3, 5, 7, 10, 20 km) [4]. The choice of optimal spectral band for thermal signature determination is generally determined by a consideration of threat signature characteristics and anticipated clutter conditions as well as scenario aspects. In this mode, the studies show us that when we will desire ground target detection, the 3- to 5 μm band provides better signal-to-noise ratios than the 8- to 12 μm band [5]. Understanding the impact of Thermal Imaging Cameras (TIC) display image quality on a fire fighter's ability to perform a hazard recognition task, test subjects were employed to identify a fire hazard by observing infrared images, the interactions between contrast, spatial resolution, brightness, and noise in an image have a greater effect on human perception than any one variable by itself. TIC can be able to produce a quality image, interactions must be accounted for, the relationship between TIC image quality and fire fighter task performance was modeling [6]. Simple atmospheric corrections of airborne thermal infrared imagery for precision farming management in tropical areas. Airborne and ground acquisitions have been done twice a month around mid-day in order to obtain a large contrast of temperature between cold and hot parts of the observed site. Images were taken from 300 m to 1300 m in order to study the sensitivity of the signal to atmospheric transmission [7]. Improvements in the spectroscopic data for water vapor have significantly increased the near-infrared absorption in models of the Earth's atmosphere. The climatic effects of increased near-infrared absorption have been simulated with the latest Community Atmosphere Model (CAM3) [8]. Thermal images of a pit wall showed point temperature gradients in excess of 500 $^{\circ}\text{C m}^{-1}$ in a snowpack structure which would present only a 0.67 $^{\circ}\text{C}$ difference between two thermometers spaced 14 cm apart in the same area [9]. The thermal camera and the methods which have been used provided data with a quantitative accuracy and spatial resolution currently. This type of data may, in the future, help link modeling of metamorphism and thin temperature gradients to the same occurrences in the natural snow cover. The aim of this paper is to study the effect of concentration of suspended dust and water vapor on thermal imaging in Karbala city depending on the experimental data which is storage in Iraq Meteorological Organization and Seismology. Thermal imaging cameras (TIC) are used for different goals such as night vision and accurate thermal image are not possible if the emissivity of IR about 0.5 or lower.

3- Thermal Emission

Many reports of division of IR range have been published [3, 4] the division is commonly depending on the limits of spectral bands of IR detectors which are used. Table (1) show division of infrared radiation. In the NIR region, sunlight is the primary source of the radiation, while reflected sunlight have a negligible effect on LWIR region, it is import- ant in the MWIR region.

Table (1) division of infrared radiation.

Region(abbreviation)	Wave length range [μm]
Near infrared (NIR)	0.78–1
Short wavelength IR (SWIR)	1-3
Medium wavelength IR (MWIR)	3-6
Long wavelength IR (LWIR)	6-15
Very long wavelength IR (VLWIR)	15-1000

A thermal image arises from temperature variations or differences in emissivity within a scene. The thermal contrast is one of the important parameters for IR imaging devices. Radiant emission is usually treated in terms of the concept of blackbodies, named black bodies because they absorb all the radiation that falls on it.

The energy density $U(\lambda, T)$ in terms of wavelength as [10].

$$U(\lambda, T) = \frac{16\pi^2 \hbar c}{\lambda^5} \frac{1}{e^{2\pi \hbar c / \lambda K T} - 1} d\lambda \quad (1)$$

Eq. (1) is called Planck's radiation law

The radiative power (energy emitted per unit area per unit time for all wavelengths)

$$R = \int_0^\infty E_\lambda d\lambda \quad (2)$$

The total energy density $U(T)$ at a temperature T

$$U(T) = \int_0^\infty U(\lambda, T) d\lambda \quad (3)$$

The radiative power of a black body is related to energy density U as

$$R = \frac{1}{4} c U(\lambda, T) \quad (4)$$

Equation (3) for all wavelengths becomes

$$R = \frac{c}{4} \int_0^\infty U(\lambda, T) d\lambda \quad (5)$$

$$R = \frac{c}{4} \int_0^\infty \frac{8\pi}{\lambda^4} K T d\lambda \quad (6)$$

3-1-Choice IR Bands

The effects of atmosphere particles on IR transmittance arise the thermal atmospheric windows; there are two main atmospheric windows, 3-5 μm (MWIR) and 8-12 μm (LWIR) band [3]. LWIR band has higher sensitivity for cool objects, while the MWIR band may be more appropriate for hotter object such as engines, power generators, and combustion gases. The advantage of MWIR band is smaller diameter of the optics required to obtain a certain resolution and that some detectors may operate at higher temperatures, but the band are required larger apertures for the resolution when operating at the diffraction limit, and cooling to 77K is generally required [11].

3-2- Atmosphere Attenuation

Atmospheric gases and small particles suspended in the atmosphere will selectively attenuate the radiation from an object before it reaches an infrared sensor [4] because of four phenomena: absorption, scattering, emission and turbulence. The first two phenomena cause attenuation of propagating optical radiation; the third one adds additional radiation, and the fourth one causes distortion of the image of the emitting objects [4]. The concentration of H_2O depends significantly on altitude, season, geographic location, time of day, and is subjected to large fluctuations [12]. The amount of H_2O in the air decreases rapidly with altitude. H_2O and CO_2 are responsible for most of the absorption in the IR region at sea level [12]. Ozone, nitrous oxide, carbon monoxide and methane are less important IR absorbing constituents of the atmosphere [3].

The attenuation coefficient (μ) can be calculated according the relation [5].

$$\mu = \alpha_g + \alpha_p + \gamma_g + \gamma_p \quad (7)$$

Where $\alpha_g, \alpha_p, \gamma_g, \gamma_p$ are molecular absorption coefficient, dust absorption coefficient , Rayleigh scattering coefficient and dust scattering coefficient respectively

The effects of absorption electromagnetic will be relatively small comparing with Mie scattering, therefore, the scattering coefficient can be computed from the visibility distance and wave of the incident ray [13].

$$V = 7080 \times C^{-0.8} \quad (8)$$

Where V visibility distance, C concentration of dusts (various with altitude).

There is a direct relation between concentrations of dust and scattering coefficient due to atmospheric aerosol is [5].

$$\tau_s = \exp \left[\left(\frac{-3.91}{7080 \times C^{-0.8}} \right) \left(\frac{\lambda}{0.55} \right)^{-q} \times R \right] \quad (9)$$

Where τ_s is the transmittance , λ is the wave length, R is propagation range and q is positive constant that is value depends on the size distribution of the scattering particles(visibility) which is illustrated at the table below[14].

Table (2) values of constant q

Constant (q)	Visibility	quality of visibility
1.6	>50 [km]	high
1.3	6[km]< V <50 [km]	average
$0.585V^{1/2}$	V <6[km]	low
V - 0.5	0.5[km] <V <1km	low
0	V <0.5 [km]	low

3. Results and Discussions

The experimental data of dust and water vapor which are recorded by Iraq Meteorological Organization and Seismology about Karbala city(see table 3&4) are considered in calculating the effects of dust and water vapor on visibility range and transmission of IR respectively . Equation (9) which is programming into Fortran 90 that is used to calculate the effect of water vapor concentration in Karbala city on IR transmission at different range in atmosphere ,this calculation give prediction for the quality of thermal image. In this program the value of the constant ($q=0.585 V^{1/2}$ see table 2) which is depending on the value of visibility, at this work the maximum value is 1954m (Fig.1)

Table (3) Concentration of dust at Karbala city in seven months of year 2013

STATION:- KARBALLA				
MONTH	MAX.TEMP.(°C)	DUST STORM	RISING DUST	SUSPENDED DUST
MAR.	23.1	2	8	18
APR.	33.1	1	10	19
MAY.	38.1	3	5	21
JUN.	43.2	0	14	24
JUL.	46.0	0	4	11
AUG.	44.3	0	6	12
SEP.	41.1	0	3	5

Table (4) Amount of monthly evaporation total (mm) at Karbala city in nine months of year 2013

STATION: KARBALA

ELEMENT: MONTHLY EVAPORATION TOTALS (mm)

YEAR	JAN.	FEB.	MAR.	APR.	MAY.	JUN.	JUL.	AUG.	SEP.	OCT.	NOV.	DEC.
2013	59.1	97.4	167	222.7	310.7	395.4	432.9	388.7	300.2			

For understanding the effect of concentration of dust on visibility range, eq. (2) have been used due to the values of dust in table(3) , (Fig. 1) shows that increase in concentration of dust (see table 3 coulomb 5) leads to decrease in visibility, there is no signal for bad visibility in 2013 at Karbala city due to maximum value of suspend particle in JUN. $24\mu\text{g}/\text{m}^3$ which gives visibility range 557m. This calculation shows a good visibility in above time and place. The national limitation of suspend particle is $350\mu\text{g}/\text{m}^3$.

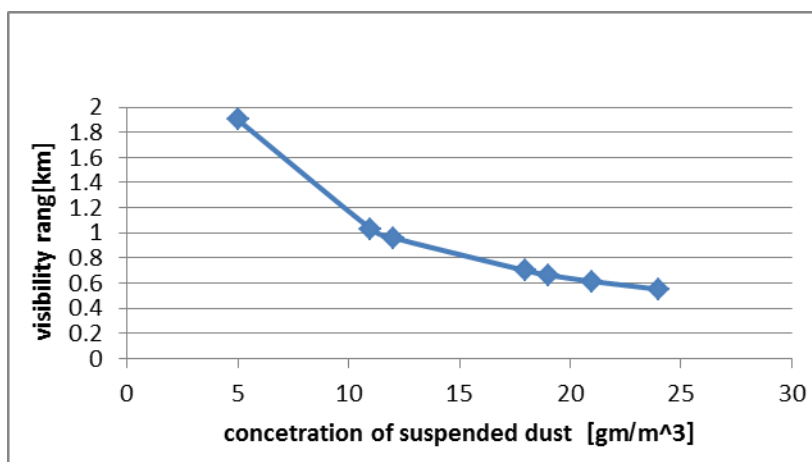


Fig.(1) effect of dust concentration on visibility in 2013 at Karbala city

The Figures (2, 3, 4) below show the IR transmission at the atmosphere with different vapor water concentrations which are considered as monthly average values of Karbala city (see table 4) ,it is clear that the transmission decreases as the concentration of water vapor increased also the horizontal path of IR transmission at the atmosphere has the same effect in case of increment. Fig.(2) series1 and 2 have simple effect and transmission can be created thermal image but series 3 has clear effect(low transmission) in the cases of high concentration of water vapor, also the same result is obtained in figures(3,4)except the first and second value of transmission further increased in distance lead to degradation in transmission until the thermal image does not detect. Figures 5,6 also illustrated IR transmission at the same input experimental data but the wave length is $3\mu\text{m}$,low transmission is obtained when it compared to $5\mu\text{m}$ wave length.

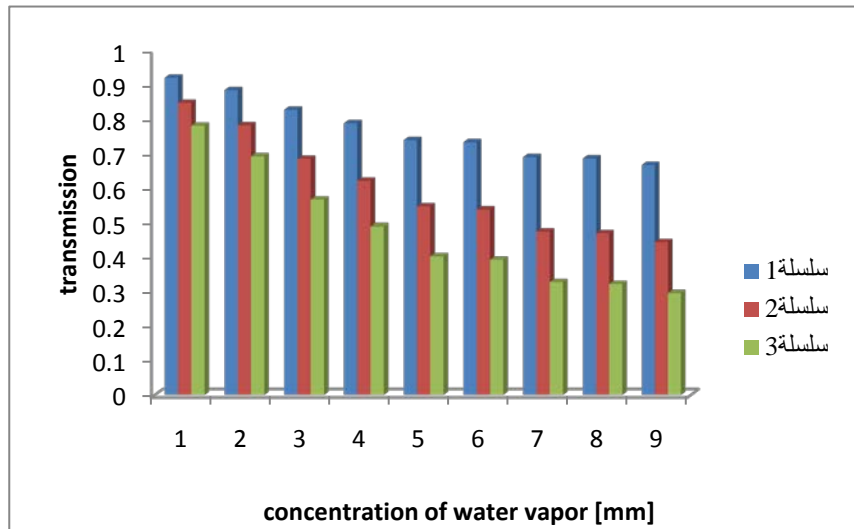


Fig.(2) Effect of water vapor on 5μm IR transmission at different Distance (series1 100m, Series2 200m, series3 300m)

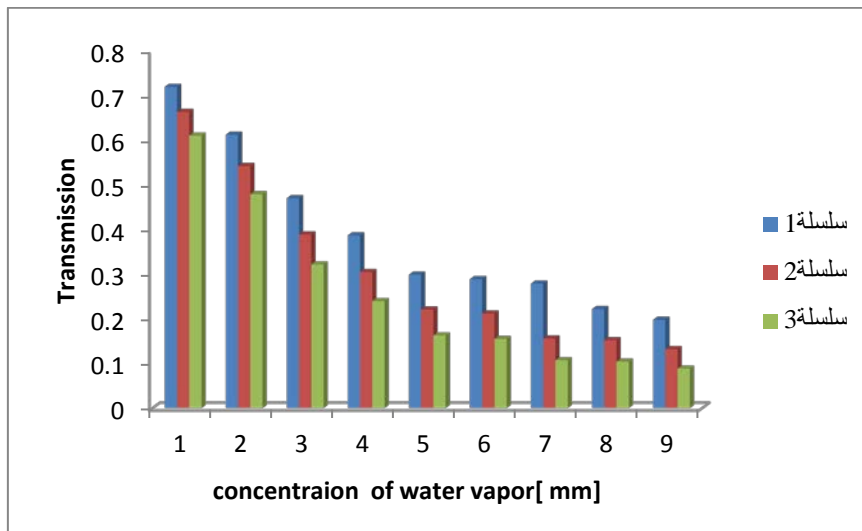


Fig. (3)Effect of water vapor on 5μm IR transmission at different Distance (series1 400m, Series2 500m, series3 600m)

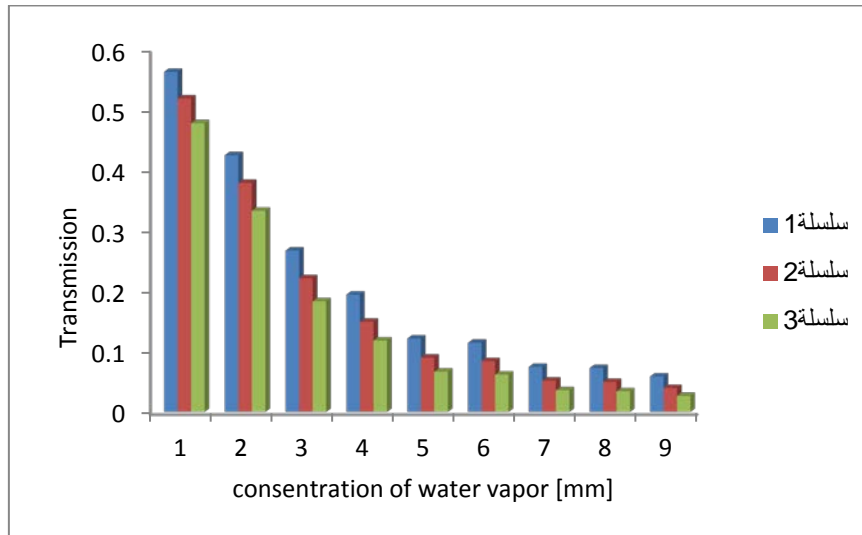


Fig.(4)Effect of water vapor on 5μm IR transmission at different Distance (series1 700m, Series2 800m, series3 900m)

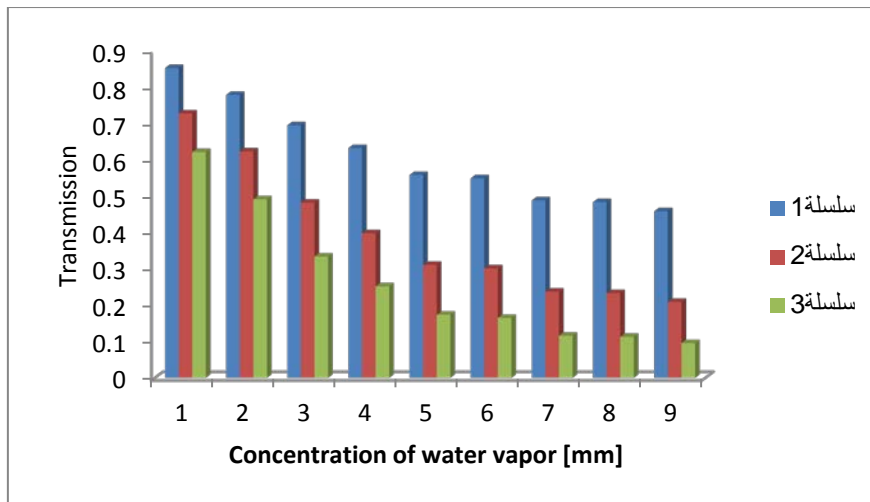


Fig.(5)Effect of water vapor on 3μm IR transmission at different Distance (series1 100m, Series2 200m, series3 300m)

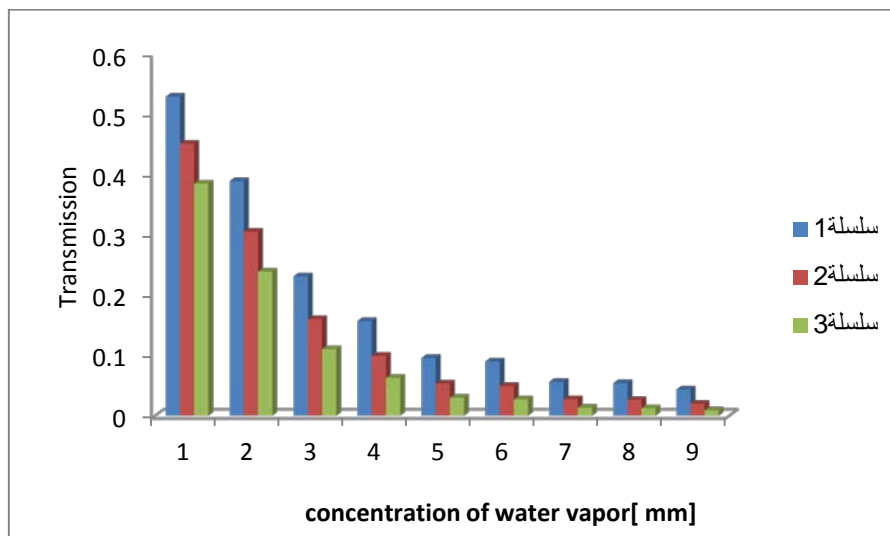


Fig.(6)Effect of water vapor on 3μm IR transmission at different Distance (series1 400m, Series2 500m, series3 600m)

4- Conclusions

- 1-The low dust concentration 5-24 [gm/m³] does not affect the visibility due to eq.(2) and calculation in Fig(1) .
- 2-high concentration of water vapor 388.7, 395.4, and 432.9 [mm] at horizontal range 200 [m] enhanced absorption of near-infrared radiation or lower transmission obtained (less than 0.5), then the thermal imaging is bad.
- 3- The resolution of the thermal image decreases with horizontal path (range) increased.
- 4- Longer wavelength range improves image resolution.

5-References

- 1- Jessica Ward law, Maciej Gryka ,Fabian Wanner ,Gabriel Brostow and Jan Kautz , A New Approach to Thermal Imaging Visualization, Thermal Imaging in 3D,University College London, ENGD Group Project ,July 30, (2010).
- 2- Infrared Training Centre (ITC),FLIR Systems AB, Thermal imaging guidebook for industrial applications, (2011).
- 3-A. Rogalski and K. Chrzanowski,Infrared devises and techniques, Opt-Electronics Review 10(2), 111–136 (2002).
- 4 -Fatten Shaqur Zain Al-Abedeem, Atmosphere Effects on 3-5 μm Band Thermal Imaging Ph.D., Al-Mustanseriya University, November, (2004).
- 5-C.Plesa,D.Țurcanu, V.Bodoc, The use of Infrared Radiation for Thermal Signatures Determination of Ground Targets, Rom. Jour. Phys.,Vol.51, Nos. 1–2, P.63–72, Bucharest, (2006).
- 6- Justin Lawrence Rowe, The Impact of Thermal Imaging Camera Display Quality on Fire Fighter Task Performance National Institute of Standards and Technology, U.S. Department of Commerce June (2009).
- 7- V. Lebourgeois, S. Labbe, F. Jacob, A. Begue, Atmospheric Corrections of Low Altitude Thermal Infrared Airborne Images Acquired Over A Tropical Cropped Area , France,(2007).
- 8- William D. Collins, Julia M. Lee-Taylor, David P. Edwards, and Gene L. Francis, Effects of increased near-infrared absorption by water vapor on the climate system, Journal of Geophysical Research, Vol. 111, D18109, doi:10.1029/2005JD006796, (2006).
- 9- C. Shea, B. Jamieson and K. W. Birkeland, Use of a thermal imager for snow pit temperatures, Copernicus Publications on behalf of the European Geosciences Union, the Cryosphere, 6, 287–299,(2012).
- 10-R.B. Singh,introduction to modern physics, volume 1, second edition ,(2009).
- 11-S.G. Burnay, T.L. Williams and G.H. Jones, “Applications of Thermal Imaging”, Adam Hilge, Bristol and Philadelphia Ltd., USA, (1988).
- 12-R.D. Hudson, John Wiely and Sons, “Infrared System Engineering”, (1969).
- 13- Korevaar E.,Kim I., and Arthur B., Debunking the recurring myth of a magic wavelength for free-space optics SPIE Journal ,Vol. 4873,P.155-161,(2002).
- 14-Kozachenko E.,and Anderson M.,A Free Space Optical Communications System,IEEE Journal ,Vol. 1,No. 3,P.195-201,(2011).